Available online at www.sciencedirect.com

ScienceDirect

Mendeleev Commun., 2024, **34**, 34–38

Mendeleev Communications

Suzuki–Miyaura cross-coupling reaction catalyzed by [R_3Si–IPr]Pd complexes: a computational study

Toru Matsui,*[a] Jun Fujiwara,[a] Norihisa Fukaya[b] and Vladimir Ya. Lee*[a]

[a] *Department of Chemistry, Faculty of Pure and Applied Sciences, University of Tsukuba, Tsukuba 305-8571, Ibaraki, Japan. E-mail: matsui@chem.tsukuba.ac.jp, leevya@chem.tsukuba.ac.jp*
[b] *National Institute of Advanced Industrial Science and Technology, Tsukuba 305-8565, Ibaraki, Japan*

DOI: 10.1016/j.mencom.2024.01.011

The cross-coupling reaction of chlorobenzene and phenylboronic acid, catalyzed by the [R_3Si–IPr]Pd^0 species (generated upon activation of {[R_3Si–IPr]Pd(η^3-allyl)Cl} pre-catalyst complexes) in the presence of hydroxide ion as a base, was studied in details by the quantum chemical calculations. Each step of the whole process, including pre-catalyst activation, oxidative addition, transmetalation and reductive elimination, were computationally probed to locate reaction intermediates and transition states along the reaction coordinate. Accordingly, transmetalation was found to be a limiting step of the catalytic cycle (involving oxidative addition, transmetalation and reductive elimination), whereas pre-catalyst activation was revealed as a limiting step of the whole catalytic process.

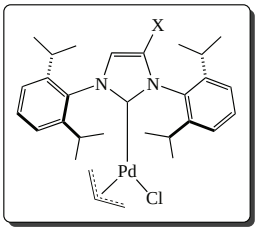

X = $SiMe_2R$ (R = Me, All, Ph, $SiMe_3$, Bu^t); $Si(OEt)_3$; H

Keywords: catalytic cycle, DFT calculations, oxidative addition, reductive elimination, transmetalation, Suzuki–Miyaura reaction, cross-coupling.

This paper is dedicated to the 70th anniversary of Professor Mikhail Egorov, Academician of the Russian Academy of Sciences, a world-leading expert in organic and organometallic chemistry.

The Suzuki–Miyaura cross-coupling reaction, that is transition metal-catalyzed coupling of organic halides and organoboronic acids, is among the most fundamental methods for the palladium-catalyzed C–C bond formation, allowing preparation of biaryls that are widely used in pharmaceutical and agricultural chemistry.[1–4] The mechanism of Suzuki–Miyaura reaction was previously comprehensively studied to address peculiarities of the reaction pathways in each step of the catalytic cycle, namely, oxidative addition, transmetalation and reductive elimination.[5–8]

Complexes {[IPr]Pd(η^3-allyl)Cl}, where IPr is 1,3-bis(2,6-diisopropylphenyl)imidazol-2-ylidene, were recently shown to be very effective pre-catalysts in the Suzuki–Miyaura reactions due to their high propensity to readily generate {[IPr]Pd^0} catalytically active species.[6,9–14] Based on our silyl-substituent modified IPr ligands [R_3Si–IPr], we recently synthesized a series of novel palladium complexes {[R_3Si–IPr]Pd(η^3-allyl)Cl} **1Pd**–**6Pd** (Figure 1), which served as excellent pre-catalysts for both Buchwald–Hartwig amination[15] and Suzuki–Miyaura cross-coupling reaction.[16] The catalytic performance of complexes **1Pd**–**6Pd** remarkably outperformed that of the commercially available {[IPr]Pd(η^3-allyl)Cl} complex **7Pd** in terms of the reaction conditions (catalyst loading, reaction temperature, reaction time) and the reaction scope. In this communication, we report our detailed computational study† on the mechanism of the Suzuki–Miyaura cross-coupling reaction using pre-catalyst complexes **1Pd**–**7Pd**. At first, the potential energy profiles were calculated for all steps of the catalytic cycle (namely, oxidative addition, transmetalation, and reductive elimination), and finally, the reaction pathway for the initial pre-catalyst activation was computationally approached to complete the whole catalytic process investigation.

Oxidative addition is the first step of the whole process, initiated after catalytically active Pd^0 species enters the

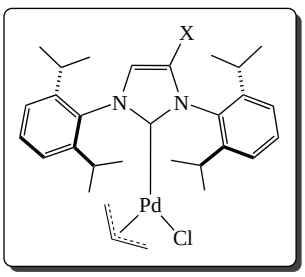

1Pd X = $SiMe_3$
2Pd X = $Si(OEt)_3$
3Pd X = $SiMe_2(CH_2CH{=}CH_2)$
4Pd X = $SiMe_2Ph$
5Pd X = $SiMe_2(SiMe_3)$
6Pd X = $SiMe_2Bu^t$
7Pd X = H

Figure 1 Palladium pre-catalysts studied in this work: our complexes **1Pd**–**6Pd** and commercial complex **7Pd** (used for comparison of catalytic performance).

† All quantum chemical calculations were performed at the DFT B3LYP level of theory with Lanl2DZ basis set (for Pd atoms) and 6-31G(d) basis set (for atoms of other elements), using GAUSSIAN16 C.01 program package (see Online Supplementary Materials for details).

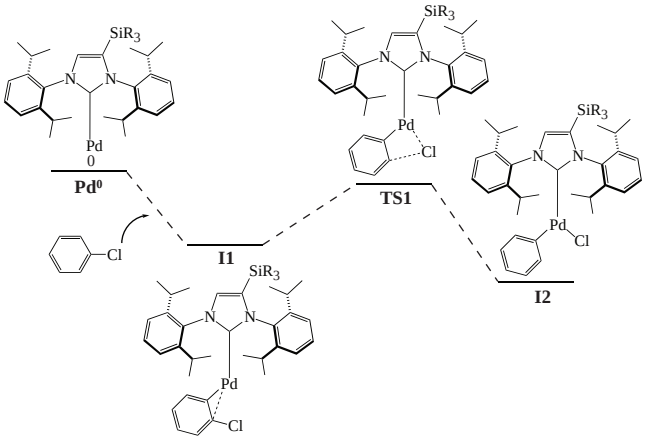

Figure 2 Reaction pathway for the oxidative addition step.

catalytic cycle, and is frequently considered as the limiting step of the Suzuki–Miyaura cross-coupling. In our computations, we employed $[R_3Si–IPr]Pd^0$ as the catalytic species, chlorobenzene as the reactant, and hydroxide ion as the base (details of our quantum-chemical calculations are given in the Online Supplementary Materials). The reaction pathway for the oxidative addition step, using complexes **1Pd**–**7Pd** as the pre-catalysts, is shown in Figure 2. At the initial stage of the process, chlorobenzene molecule approaches the catalytically active species $[R_3Si–IPr]Pd^0$, forming η^2-Pd-complex across one of the C–C bond of arene and generating intermediate **I1**. Due to their close spatial proximity in **I1**, Cl atom gradually approaches Pd center through the transition state **TS1** to the final intermediate **I2** in which Pd is η^1-coordinated to both Ph and Cl groups (see Figure 2). According to this reaction pathway, oxidative addition proceeds in a concerted manner with quite low activation energy consistent with the room temperature process, ranging from 8.04 to 8.54 kcal mol^{-1} and thus being within 0.5 kcal mol^{-1} difference (all energies discussed in this study include zero-point energy correction) for the pre-catalysts **1Pd**–**7Pd** which all showed high performance at the oxidative addition step (Table 1).

Table 1 Comparison of energies (kcal mol^{-1}) for each reaction state and activation energy (E_a) for the oxidative addition step, using pre-catalyst complexes **1Pd–7Pd**.

Complex	**Pd^0**	**I1**	**TS1**	**I2**	E_a^{TS}
1Pd	0	–10.75	–2.71	–18.42	8.04
2Pd	0	–10.60	–2.44	–17.40	8.15
3Pd	0	–11.93	–3.67	–18.88	8.27
4Pd	0	–10.60	–2.05	–16.85	8.54
5Pd	0	–10.69	–2.57	–17.47	8.11
6Pd	0	–10.70	–2.61	–17.76	8.09
7Pd	0	–10.78	–2.43	–16.79	8.35

We assume that at the transmetalation step, the phenylboronic acid $PhB(OH)_2$, hydroxide ion $OH^–$ as a base, and the oxidative addition product **I2** (see Figure 2) are present in the reaction mixture. Poater and co-workers reported that the Suzuki–Miyaura cross-coupling is initiated not by the direct coordination of $OH^–$ to palladium but by the coordination of $[PhB(OH)_3]^–$ generated *via* the initial attack of $OH^–$ on $PhB(OH)_2$ to palladium instead.[6] Therefore, one can expect a similar reaction pathway in our catalytic system as well. According to our studies, in the first step $[PhB(OH)_3]^–$ species coordinates to palladium *via* the O atom of one of its hydroxy ligands, generating intermediate **I3** featuring four-coordinate palladium center (Figure 3). Then, another OH-group of the borate ligand in **I3** comes closer to palladium, gradually expelling chloride ligand from the coordination sphere of transition metal, and thus generating transition state **TS2**. Elimination of $Cl^–$ converts **TS2** into very stable four-membered ring palladacycle intermediate **I4**. Then, Ph-group of the borate ligand comes to the close proximity of Pd environment partially coordinating *via* its *ipso*-C, and at the same time one of the OH-groups of borate ligand moves away from palladium coordination, generating transition state **TS3** (see Figure 3).

The complete breaking of one of the Pd–OH bonds in **TS3** results in the intermediate **I5**. The subsequent bond reorganization (stretching of the C–B bond) transforms **I5** to the transition state **TS4** (see Figure 3). The transmetalation step is completed by the

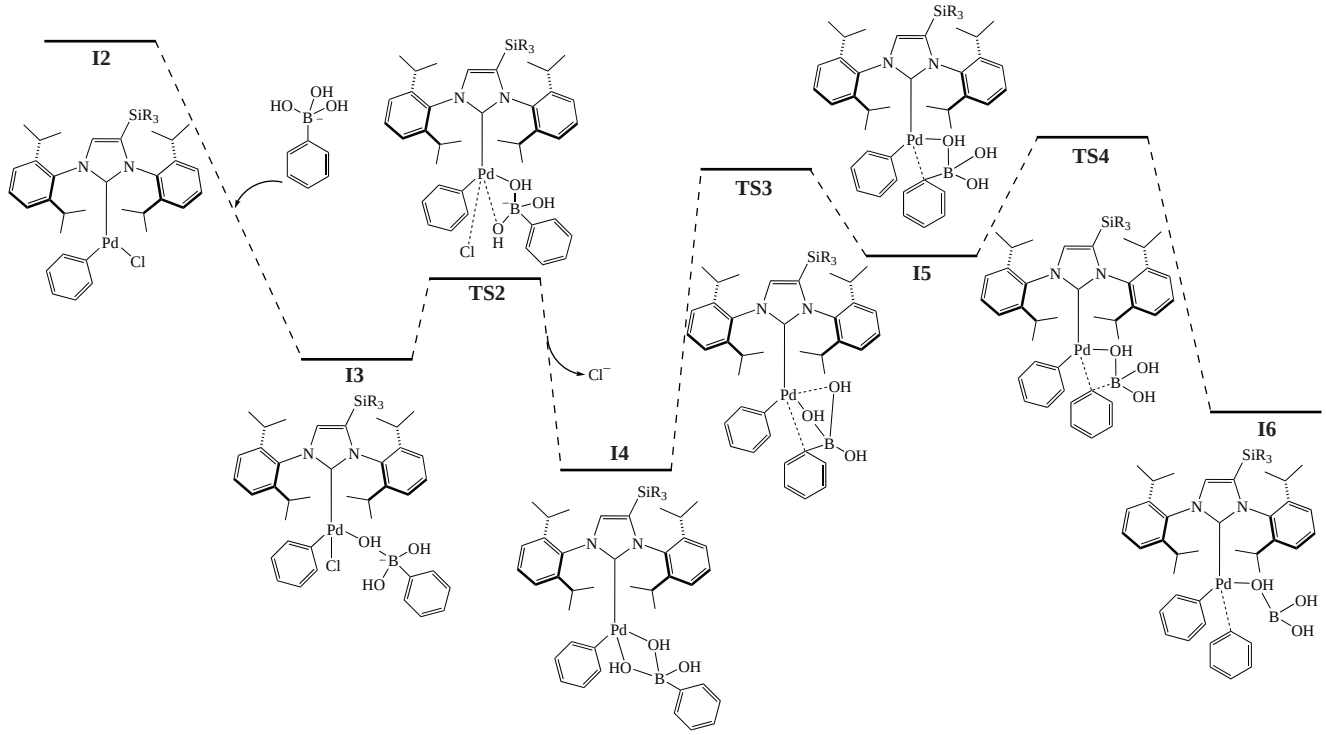

Figure 3 Reaction pathway for the transmetalation step.

breaking of the B–C bond and formation of the Pd–C(aryl) bond, generating the final intermediate **I6**. For all pre-catalyst complexes studied, **1Pd–7Pd**, the highest activation energy is the one leading to **TS3**, which implies that the limiting step of transmetalation is the one converting **I4** to **TS3** (Tables 2 and 3). Again, the difference in E_a^{TS3} is within *ca.* 2 kcal mol^{-1} for all complexes **1Pd–7Pd**, implying that all of them perform quite comparably at the transmetalation step.

At the reductive elimination step, the two aryl groups, each coordinated to palladium at the oxidative addition step and transmetalation step, respectively, are eliminated to form biaryls upon reduction of palladium from +2 to 0. At this stage, the initial catalytically active [R_3Si–IPr]Pd^0 species is regenerated to initiate the next catalytic cycle by its reaction with aryl halide. At the reductive elimination step, two aryl groups must be in a close proximity to each other to enable formation of the C–C bond between them. And indeed, in the final intermediate of transmetalation **I6**, the two aryl groups are coordinated to palladium in *cis*-fashion, thus facilitating their bonding interaction.

The initial process of the reductive elimination step is removal of boronic acid B(OH)$_3$ away from palladium center (Figure 4). The mutual *cis*-arrangement of the two aryl groups at Pd in the resulting intermediate **I7** is maintained upon elimination of boronic acid. Then, the two aryl groups at palladium in **I7** closely approach each other, which stimulates formation of a partial bonding between them (*ipso*-C–*ipso*-C bonding) and generation of transition state **TS5** (see Figure 4). Finally, biphenyl (as a cross-coupling reaction product) is eliminated from the coordination sphere of palladium, and [R_3Si–IPr]Pd^0 is regenerated (as a catalytically active species).

Table 2 Comparison of energies (kcal mol^{-1}) for each reaction state for the transmetalation step, using pre-catalyst complexes **1Pd**–**7Pd**.

Complex	**I3**	**TS2**	**I4**	**TS3**	**I5**	**TS4**	**I6**
1Pd	–40.78	–36.23	–47.14	–32.17	–34.37	–27.92	–43.84
2Pd	–39.42	–35.94	–45.96	–29.66	–34.01	–27.11	–41.28
3Pd	–40.60	–36.61	–47.03	–32.46	–34.43	–28.06	–43.84
4Pd	–35.91	–34.37	–44.95	–30.27	–32.51	–25.72	–41.85
5Pd	–38.43	–34.32	–44.66	–29.54	–29.55	–26.11	–41.87
6Pd	–35.40	–33.87	–44.67	–29.35	–32.75	–25.96	–41.51
7Pd	–44.08	–39.79	–48.87	–34.59	–36.52	–30.02	–45.43

Table 3 Activation energy (kcal mol^{-1}) for the three transition states (**TS2**, **TS3**, **TS4**).

Complex	E_a^{TS2}	E_a^{TS3}	E_a^{TS4}
1Pd	4.56	14.96	6.45
2Pd	3.48	16.30	6.91
3Pd	3.99	14.57	6.37
4Pd	1.54	14.68	6.79
5Pd	4.12	15.11	6.92
6Pd	1.53	15.32	6.79
7Pd	4.29	14.28	6.50

As can be seen from Table 4, reductive elimination readily proceeds for all pre-catalysts **1Pd**–**7Pd** with quite low activation energies of 2.18–5.00 kcal mol^{-1}, whose values are remarkably smaller than those for the oxidative addition and transmetalation steps, indicating that the reductive elimination has a little impact on the overall course of the Suzuki–Miyaura cross-coupling reaction.

Pre-catalyst activation step begins with a substitution of hydroxide ion (as a base) for a chloride ligand in the pre-catalyst Pd^{II} in a highly exergonic spontaneous process forming intermediate **I8** (Figure 5). In **I8**, the hydroxide ligand gradually approaches allyl ligand (with a partial bonding between them), at the same time gradually leaving Pd center with stretching of the Pd–O bond, thus generating transition state **TS6**. Upon going from the **TS6** to the intermediate **I9**, the Pd–O bond is completely cleaved and the novel allyl–O bond is formed, which is accompanied by the change in the [Pd–allyl ligand]-coordination mode from η^3 to η^2. Finally, allyl alcohol leaves the palladium center, thus generating a catalytically active species Pd^0 (see Figure 5).

Table 4 Comparison of energies (kcal mol^{-1}) for each reaction state for the reductive elimination step, using pre-catalyst complexes **1Pd**–**7Pd**.

Complex	**I6**	**I7**	**TS5**	**Pd^0**	E_a^{TS5}
1Pd	–43.84	–44.69	–40.68	–62.95	4.01
2Pd	–41.28	–43.58	–38.77	–62.95	4.81
3Pd	–43.84	–45.37	–40.71	–62.95	4.66
4Pd	–41.85	–43.69	–39.22	–62.95	4.46
5Pd	–41.87	–41.48	–39.30	–62.95	2.18
6Pd	–41.51	–44.30	–39.56	–62.95	4.74
7Pd	–45.43	–44.77	–39.77	–62.95	5.00

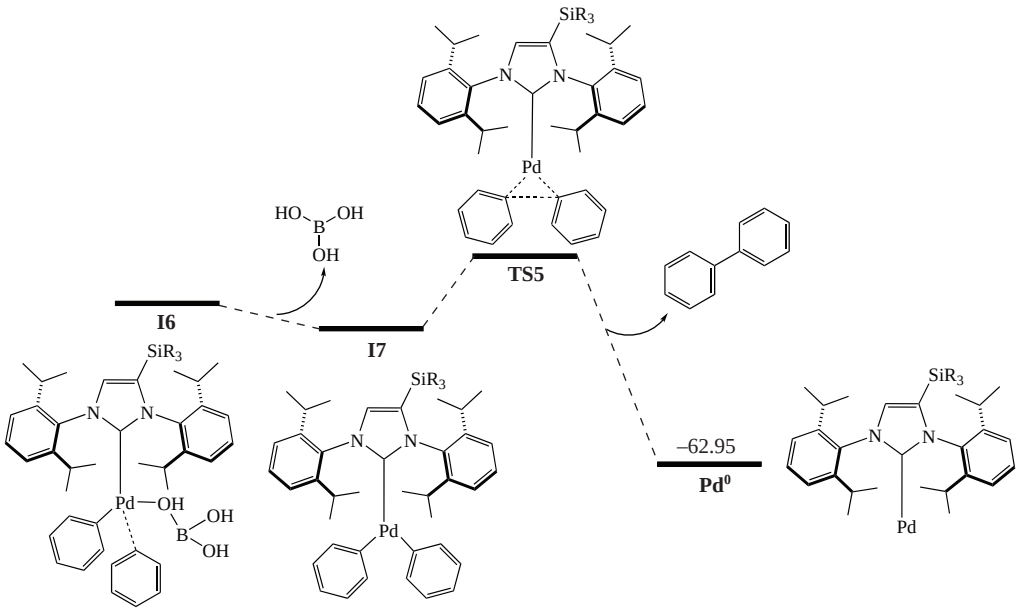

Figure 4 Reaction pathway for the reductive elimination step.

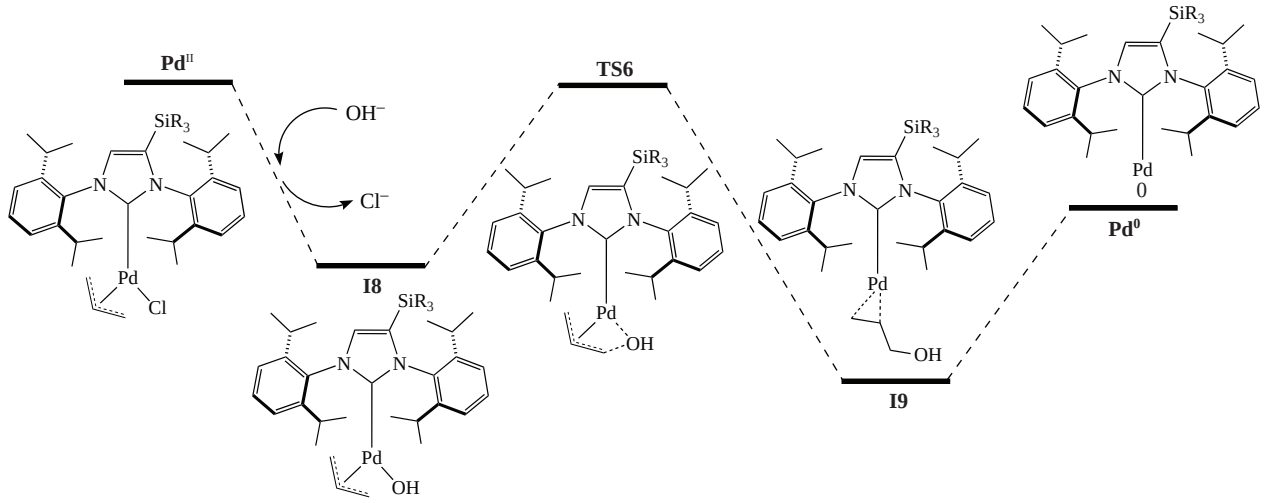

Figure 5 Reaction pathway for the pre-catalyst activation step.

The lowest activation energy (23.80 kcal mol^{-1}) was found for **2Pd** pre-catalyst, whereas the highest activation energy (26.71 kcal mol^{-1}) was calculated for the parent complex {[IPr]Pd(η^3-allyl)Cl} **7Pd** lacking silyl-substituents at the NHC ligand (Table 5). Overall, the activation energies given in Table 5 (pre-catalyst activation) are notably greater than those in Table 1 (oxidative addition), Table 3 (transmetalation), and Table 4 (reductive elimination). This implies that transmetalation is the limiting step of the catalytic cycle (oxidative addition–transmetalation–reductive elimination), whereas pre-catalyst activation is the limiting step of the whole catalytic process that starts with the pre-catalyst activation generating catalytically active Pd^0 species [R_3Si–IPr]Pd^0, which then enters the catalytic cycle at the initial oxidative addition step.

The oxidative addition is commonly considered as the rate-determining step in the Suzuki–Miyaura cross-coupling reaction catalytic cycle, although transmetalation and reductive elimination are also sometimes proposed as the limiting steps.[17] However, it is now getting more and more clear that the overall picture of Suzuki–Miyaura reaction catalyzed by Pd complexes is incomplete without consideration of the pre-catalyst activation step as the initial stage of the whole catalytic process, whose critical importance has been recently acknowledged.[6] In our comprehensive study on the whole catalytic process of the Suzuki–Miyaura reaction with {[R_3Si–IPr]Pd(η^3-allyl)Cl} complexes as pre-catalysts (pre-catalyst activation, oxidative addition, transmetalation, and reductive elimination steps), we found that the limiting step of the catalytic cycle was the transmetalation reaction, whereas the limiting step of the whole catalytic process was the pre-catalyst activation step. Accordingly, our investigations confirm the crucial importance of the pre-catalyst activation step, generating the catalytically active Pd^0 species that enter and start the catalytic cycle. In accord with our preliminary computational studies,[16] our pre-catalyst R_3Si-substituted Pd-complexes **1Pd**–**6Pd** exhibited remarkably better catalytic performance compared to the commercially available complex **7Pd** because of the weaker interaction between the Pd center and the attached hydroxyl ligand in the intermediate **I8** (in **1Pd**–**6Pd**, compared to **7Pd**), facilitating subsequent cleavage of the Pd–OH bond and thus reducing the activation barrier on going from **I8** to **TS6** (23.80–25.63 kcal mol^{-1} for **1Pd**–**6Pd** *vs.* 26.71 kcal mol^{-1} for **7Pd**) on the way to generate the catalytically active Pd^0 species.

Table 5 Comparison of energies (kcal mol^{-1}) for each reaction state for the pre-catalyst **1Pd**–**7Pd** activation step.

Complex	**Pd^{II}**	**I8**	**TS6**	**I9**	**Pd^0**	E_a^{TS6}
1Pd	11.62	–13.60	11.88	–24.38	0	25.48
2Pd	13.85	–11.99	11.81	–22.32	0	23.80
3Pd	11.57	–13.79	11.85	–24.59	0	25.63
4Pd	13.44	–12.04	13.05	–22.92	0	25.09
5Pd	14.49	–11.81	13.11	–23.04	0	24.91
6Pd	14.59	–11.61	12.94	–23.38	0	24.55
7Pd	12.13	–12.24	14.47	–20.24	0	26.71

This work is partially supported by the JSPS KAKENHI Grants program (nos. JP21K05017, 19K05381) from the Ministry of Education, Science, Sports, and Culture of Japan. The computation was performed using Research Center for Computational Science, Okazaki, Japan (Project: 21-IMS-C075). The contribution of Prof. Kenji Morihashi, who supervised the research work of Jun Fujiwara during his Master course studies at the University of Tsukuba in 2019–2020, is also gratefully acknowledged.

Online Supplementary Materials

Supplementary data associated with this article can be found in the online version at doi: 10.1016/j.mencom.2024.01.011.

References

1 N. Miyaura and A. Suzuki, *Chem. Rev.*, 1995, **95**, 2457.
2 A. Suzuki, *J. Organomet. Chem.*, 1999, **576**, 147.
3 A. Suzuki, *J. Organomet. Chem.*, 2002, **653**, 83.
4 A. J. J. Lennox and G. C. Lloyd-Jones, *Chem. Soc. Rev.*, 2014, **43**, 412.
5 A. A. C. Braga, N. H. Morgon, G. Ujaque and F. Maseras, *J. Am. Chem. Soc.*, 2005, **127**, 9298.
6 G. M. Meconi, S. V. C. Vummaleti, J. A. Luque-Urrutia, P. Belanzoni, S. P. Nolan, H. Jacobsen, L. Cavallo, M. Solà and A. Poater, *Organometallics*, 2017, **36**, 2088.
7 A. A. Thomas, A. F. Zahrt, C. P. Delaney and S. E. Denmark, *J. Am. Chem. Soc.*, 2018, **140**, 4401.
8 F. Izquierdo, C. Zinser, Y. Minenkov, D. B. Cordes, A. M. Z. Slawin, L. Cavallo, F. Nahra, C. S. J. Cazin and S. P. Nolan, *ChemCatChem*, 2018, **10**, 601.
9 M. S. Viciu, R. F. Germaneau, O. Navarro-Fernandez, E. D. Stevens and S. P. Nolan, *Organometallics*, 2002, **21**, 5470.
10 M. S. Viciu, R. F. Germaneau and S. P. Nolan, *Org. Lett.*, 2002, **4**, 4053.
11 O. Navarro, H. Kaur, P. Mahjoor and S. P. Nolan, *J. Org. Chem.*, 2004, **69**, 3173.
12 M. S. Viciu, O. Navarro, R. F. Germaneau, R. A. Kelly, III, W. Sommer, N. Marion, E. D. Stevens, L. Cavallo and S. P. Nolan, *Organometallics*, 2004, **23**, 1629.
13 J. D. Egbert, A. Chartoire, A. M. Z. Slawin and S. P. Nolan, *Organometallics*, 2011, **30**, 4494.

14 N. Marion, O. Navarro, J. Mei, E. D. Stevens, N. M. Scott and S. P. Nolan, *J. Am. Chem. Soc.*, 2006, **128**, 4101.
15 N. Fukaya, T. Mizusaki, K. Hatakeyama, Y. Seo, Y. Inaba, K. Matsumoto, V. Ya. Lee, Y. Takagi, J. Kuwabara, T. Kanbara, Y.-K. Choe and J.-C. Choi, *Organometallics*, 2019, **38**, 375.
16 Y. Seo, W. S. Putro, M. Faried, V. Ya. Lee, T. Mizusaki, Y. Takagi, Y.-K. Choe, K. Matsumoto, J.-C. Choi and N. Fukaya, *J. Organomet. Chem.*, 2021, **954**–**955**, 122096.
17 M. Busch, M. D. Wodrich and C. Corminboeuf, *ACS Catal.*, 2017, **7**, 5643.

Received: 30th October 2023; Com. 23/7291